

Staying Thermal with Hartree Ensemble Approximations

Mischa Sallé* Jan Smit[†] and Jeroen C. Vink[‡]

Institute of Theoretical Physics, University of Amsterdam,
Valckenierstraat 65, 1018 XE Amsterdam, The Netherlands.

arXiv:hep-ph/0012362v2 28 Aug 2001

Abstract

We study thermal behavior of a recently introduced Hartree ensemble approximation, which allows for non-perturbative inhomogeneous field configurations as well as for approximate thermalization, in the φ^4 model in 1+1 dimensions. Using ensembles with a free field thermal distribution as out-of-equilibrium initial conditions we determine thermalization time scales. The time scale for which the system stays in approximate quantum thermal equilibrium is an indication of the time scales for which the approximation method stays reasonable. This time scale turns out to be two orders of magnitude larger than the time scale for thermalization, in the range of couplings and temperatures studied. We also discuss simplifications of our method which are numerically more efficient and make a comparison with classical dynamics.

* e-mail: msalle@science.uva.nl

† e-mail: jsmit@science.uva.nl

‡ e-mail: jcvink@science.uva.nl

1 Introduction

It is highly desirable to be able to numerically simulate quantum field dynamics in real time. This will give an important tool for the study of non-perturbative phenomena in out-of-equilibrium systems, such as phase transitions in the early universe or the quark-hadron transition in heavy-ion collisions. Using real time dynamics may also offer an alternative to simulating equilibrium physics, just like molecular dynamics simulations provide a fruitful alternative to Monte Carlo simulations in other areas of physics. Simulating quantum fields in real time is very difficult. Direct approaches, such as solving the Schrödinger equation for the field wave-functional or evaluating the Minkowski path integral using Monte Carlo methods, are prohibitively time-consuming. One has to resort to approximate methods, of which the classical approximation (see e.g. [1–10]), the Hartree approximation and large n methods (see e.g. [11, 12, 13]) are most commonly used.

In the classical approximation one assumes that the fields follow classical equations of motion. This is reasonable when the occupation numbers of the field quanta are large, but in field theory this is never the case for all modes. For instance, at high temperatures the low momentum modes of the fields are highly occupied and follow the classical Boltzmann distribution, but at large momenta occupation numbers are low and the classical distribution differs significantly from the quantum Bose-Einstein distribution, giving rise to Rayleigh-Jeans divergences.

These divergences are absent in the Hartree and large n approximations, which include quantum effects in the field dynamics. In these approximations the density operator is effectively gaussian, such that all information is contained in the mean field and two-point function. These are usually assumed to be translationally invariant. A problem which arises under these circumstances is that the system does not thermalize [11, 12], in contrast to the classical approximation which has no such problem [8]. The particles corresponding to the quantum modes of the field interact via the mean field and since this field is homogeneous there is no scattering which leads to redistribution of occupation numbers over different momentum modes and there is no thermalization. One way to amend this situation may be an improved approximation which includes direct scattering [14].

Recently we have extended the Hartree approximation by writing an initial density operator as an ensemble of coherent states with generally inhomogeneous mean fields and two-point functions. Some further discussion may be required to understand the motivation for this approach. To start, we note that there is a class of density operators $\hat{\rho}$ which can be written as a superposition of gaussian pure states (see [15, 16] and the appendix A of [17]):[§]

$$\hat{\rho} = \int [d\varphi d\pi] p[\varphi, \pi] |\varphi, \pi\rangle \langle \varphi, \pi|. \quad (1)$$

The $|\varphi, \pi\rangle$ are coherent states centered around $\varphi(\mathbf{x}) = \langle \varphi, \pi | \hat{\varphi}(\mathbf{x}) | \varphi, \pi \rangle$ and $\pi(\mathbf{x}) = \langle \varphi, \pi | \hat{\pi}(\mathbf{x}) | \varphi, \pi \rangle$, and $p[\varphi, \pi]$ is a functional representing the density operator $\hat{\rho}$.

[§] Operators are indicated with a caret.

For example, for a free scalar field the canonical distribution $\hat{\rho} = \exp(-\beta\hat{H}[\varphi, \pi])$ is represented as (see the appendix A of [17] for a derivation)

$$p[\varphi, \pi] \propto \prod_{\mathbf{k}} \exp [-(e^{\beta\omega_{\mathbf{k}}} - 1)(\pi_{\mathbf{k}}^2 + \omega_{\mathbf{k}}^2\varphi_{\mathbf{k}}^2)/2\omega_{\mathbf{k}}], \quad (2)$$

where \mathbf{k} labels the modes of the field with frequency $\omega_{\mathbf{k}}$.

By writing the density operator in this form, and we emphasize that e.g. for the canonical distribution (2) there are no approximations involved, we have achieved four things. Firstly, we have made contact with the classical approximation. If the mean field in a coherent state is large compared to the width of the state, the gaussian wavepacket approximately follows a classical trajectory and the mean field can be thought of as a *classical* field. This then suggests that the individual coherent states in the ensemble may be referred to as “realizations”. However, by using an ensemble of coherent states rather than classical fields, we have a (hopefully much) better description for those modes that have low occupation numbers for which the classical dynamics is a poor approximation. Secondly, we have expressed a (typically non-gaussian) initial density operator in terms of gaussian states. These are optimal for the Hartree method, which we want to use to approximate the dynamics of these states. Thirdly, the mean fields in the individual coherent states are *inhomogeneous*, therefore the particles can interact with the inhomogeneous mean field, such that the energy may get distributed over the full momentum range. In [17] we found that this leads to approximate thermalization in coarse grained distributions. Averaging over the initial ensemble is not necessary *per se*, since it also occurs in each individual member of the ensemble, because of coarsening over the volume, provided the volume is large enough to contain a sufficient number of decorrelated systems. Finally, there is another aspect which is relevant in this context. When non-perturbative field configurations (domain walls, skyrmions, sphalerons, etc.) play a role, these can be taken into account with inhomogeneous background fields (i.e. mean field realizations). This may also be important for thermalization.

In our previous work [17] the initial state was such that only a few of the low momenta modes of the mean field realizations carried all the energy. Such initial conditions were useful for equilibration tests. We found partial thermalization to an approximate Bose-Einstein (BE) distribution, for a limited time. Gradually the distribution also started to show classical equipartition features. For practical applications it is therefore important to get more information on the relevant time scales, and this is the main subject of this paper.

In the present work the initial energy is distributed over all momentum modes of the realizations as in (2). This initial density operator is still out of equilibrium because of interactions. As will be shown in the next sections, this leads to creation of quantum particles of all energies with a Bose-Einstein distribution. Depending on the interaction strength and temperature, this equilibrium may last for a long time before classical features begin to dominate, and we are able to better quantify the relevant time scales.

An important diagnostic in this and our previous work is the particle distribution function, which is defined in terms of equal-time two-point functions. The definition

assumes a quasi-particle picture and we check this here by performing a Monte Carlo computation in imaginary time to compute the exact two-point correlation function.

The computations of the quantum mode dynamics is numerically very expensive. Therefore we also study the effect of reducing the number of quantum field modes. With the present initial conditions in terms of a temperature $T = \beta^{-1}$ it is natural to try eliminating modes with $|\mathbf{k}| \gg T$. The often used classical approximation corresponds to the extreme of leaving out all quantum modes and to see how close this can mimic the quantum world we also make a comparison with this case. It turns out that even with a substantially reduced number of modes, this extended Hartree method fares much better than the classical approximation.

We again use the φ^4 model in $1 + 1$ dimension as a test case. This model, the Hartree ensemble approach and initial conditions are briefly recalled in Sect. 2. In Sect. 3 we recall our definition of the particle distribution in terms of equal time correlation functions and perform a Monte Carlo check on the underlying quasi-particle picture. In Sects. 4 and 5 we study equilibration time scales at weak and stronger coupling. Next, in Sect. 6, we show that the expensive computations of the quantum mode dynamics can be substantially reduced by using only a limited number of mode functions. In Sect. 7 we make a comparison with classical dynamics. Finally in Sect. 8 we discuss the results.

2 Method

2.1 Hartree ensemble approximation

Consider the Hamiltonian of a scalar field in one dimension, discretized on a lattice,

$$\hat{H} = \sum_x \left[\frac{1}{2} \hat{\pi}_x^2 - \frac{1}{2} \hat{\varphi}_x (\Delta \hat{\varphi})_x + \frac{1}{2} \mu^2 \hat{\varphi}_x^2 + \frac{1}{4} \lambda \hat{\varphi}_x^4 \right], \quad (3)$$

with $x = a, 2a, \dots, Na$, $\Delta \hat{\varphi}_x = (\hat{\varphi}_{x+a} + \hat{\varphi}_{x-a} - 2\hat{\varphi}_x)/a^2$. The volume is $L = Na$ with periodic boundary conditions; The Heisenberg equations follow as,

$$\dot{\hat{\varphi}}_x = \hat{\pi}_x, \quad \dot{\hat{\pi}}_x = (\Delta \hat{\varphi})_x - \mu^2 \hat{\varphi}_x - \lambda \hat{\varphi}_x^3. \quad (4)$$

Rather than solving the exact operators from the Heisenberg equation, we use the gaussian or Hartree approximation (see e.g. [17] for details). This amounts to approximating the field operators as linear combinations of time-*independent* creation and annihilation operators \hat{b}_α^\dagger and \hat{b}_α ,

$$\begin{aligned} \hat{\varphi}_x &= \varphi_x + \sum_\alpha [f_x^\alpha \hat{b}_\alpha + f_x^{\alpha*} \hat{b}_\alpha^\dagger], \\ \hat{\pi}_x &= \pi_x + \sum_\alpha [f_x^\alpha \hat{b}_\alpha + f_x^{\alpha*} \hat{b}_\alpha^\dagger], \end{aligned} \quad (5)$$

with time-dependent mean fields φ and π , and mode functions f^α . All information is contained in the one- and two-point functions, which can be expressed as

$$\langle \hat{\varphi}_x \rangle = \varphi_x, \quad C_{xy} = \langle \hat{\varphi}_x \hat{\varphi}_y \rangle - \langle \hat{\varphi}_x \rangle \langle \hat{\varphi}_y \rangle = \sum_\alpha [(1 + n_\alpha^0) f_x^\alpha f_y^{\alpha*} + n_\alpha^0 f_y^\alpha f_x^{\alpha*}], \quad (6)$$

and similarly for the one- and two-point functions involving $\hat{\pi}$. The n_α^0 are the particle number densities in the initial state. In our numerical work we shall take $n_\alpha^0 = 0$, such that the system is described by a pure state wave-functional. All 1PI higher-point functions are zero (i.e. higher-point functions factorize in one- and two-point functions). The mode functions represent the width of the wave-functional, allowing for quantum fluctuations around the mean field. Alternatively one can think of them as describing the particles in the model. Since the Hartree method uses (gaussian) wave-functionals, we expect to improve on the classical dynamics. Of course we cannot expect to capture all quantum effects, e.g. tunneling is beyond the scope of this gaussian approximation.

Substituting the gaussian ansatz (5) in the Heisenberg equations (4) and taking expectation values, we find self-consistent equations for the mean field φ_x and the mode functions f_x^α ,

$$\begin{aligned}\ddot{\varphi}_x &= \Delta\varphi_x - \left[\mu^2 + \lambda\varphi_x^2 + 3\lambda \sum_\alpha (2n_\alpha^0 + 1) |f_x^\alpha|^2 \right] \varphi_x, \\ \ddot{f}_x^\alpha &= \Delta f_x^\alpha - \left[\mu^2 + 3\lambda\varphi_x^2 + 3\lambda \sum_\alpha (2n_\alpha^0 + 1) |f_x^\alpha|^2 \right] f_x^\alpha.\end{aligned}\tag{7}$$

To solve these equations we use a leap-frog algorithm, which is stable for sufficiently small time steps. Since there are N mode functions (the lattice has N sites), the amount of work to progress the fields over one time-step is $O(N^2)$.

Above we described the Hartree approximation. In the Hartree ensemble method this approximation is applied to each individual realization $|\varphi, \pi\rangle\langle\varphi, \pi|$ of the initial conditions as in (1). So in eq. (6) the gaussian brackets stand for $\langle\cdot\rangle = \langle\varphi, \pi|\cdot|\varphi, \pi\rangle$ and the average over φ, π is only taken in the evaluation of observables. Furthermore these states are pure, hence the initial particle density $n_\alpha^0 = 0$ in (6) and (7).

In this way we compute correlation functions with a generally non-gaussian density operator $\hat{\rho} = \sum_i p_i |\varphi^{(i)}, \pi^{(i)}\rangle\langle\varphi^{(i)}, \pi^{(i)}|$, as

$$S_{xy} = \sum_i p_i [C_{xy}^{(i)} + \varphi_x^{(i)} \varphi_y^{(i)}] - \left(\sum_i p_i \varphi_x^{(i)} \right) \left(\sum_j p_j \varphi_y^{(j)} \right).\tag{8}$$

The $C_{xy}^{(i)}$ and $\varphi_x^{(i)}$ are computed with gaussian pure states using (6). This means that in the time-evolution the gaussian approximation is used, while expectation values are calculated using the more general initial density operator.

It should be stressed that for typical realizations the mean field $\varphi_x^{(i)}$ is *inhomogeneous* in space, in contrast to the ensemble average $\sum_i p_i \varphi_x^{(i)}$ which is in fact homogeneous for the initial conditions we shall employ. We also note that the equations (7) can be derived from a hamiltonian. Since the equations are also strongly non-linear, this might suggest that the system could evolve to an equilibrium distribution with equipartition of energy, as in classical statistical physics. On the other hand, the mode functions satisfy Klein-Gordon type orthogonality and completeness relations that could obstruct such an equipartition and it is not easy to predict the equilibrium distribution of the model [17].

2.2 Initial conditions

In order to solve the equations of motion (7), we must specify initial conditions for the mean field $\varphi^{(i)}$ and the modes $f^{\alpha(i)}$ of the individual Hartree trajectories as well as the weights p_i . This amounts to specifying the initial density operator $\hat{\rho}$. As explained in the introduction, we use coherent (pure) states to represent the initial density operator, hence we use initial modes functions as in the vacuum state (with the initial particle density n_α^0 equal to zero). The initial mode functions may be taken as plane waves with wave vector k ($\alpha \rightarrow k$), with a normalization appropriate for a zero temperature free field,

$$f_x^k(0) = \frac{e^{ikx}}{\sqrt{2\omega_k L}}, \quad \dot{f}_x^k(0) = -i\omega_k \frac{e^{ikx}}{\sqrt{2\omega_k L}}, \quad (9)$$

(the same for each realization i). L is the system size and $\omega_k = \sqrt{m^2 + [2 - 2\cos(ak)]/a^2}$, with m the zero temperature mass. We will not choose the initial φ as far out of equilibrium as we did in ref. [17]. There we took a superposition of only a few low momenta modes,

$$\varphi_x^{(i)} = v, \quad \pi_x^{(i)} = Am \sum_{j=1}^{j_{\max}} \cos(2\pi jx/L - \psi_j^{(i)}), \quad (10)$$

where $v = \sqrt{m^2/2\lambda}$ is the vacuum expectation value of the mean field in the ‘‘broken symmetry phase’’ at zero temperature and $\psi_j^{(i)}$ is a random phase. Here we choose the mean fields from an ensemble with a Bose-Einstein distribution for the φ and π momentum modes as in (2),

$$p_k(\varphi_k, \pi_k) \propto \exp[-(e^{\omega_k/T_0} - 1)(\pi_k^2 + \omega_k^2(\varphi_k - \delta_{k0}v)^2)/2\omega_k]. \quad (11)$$

Then the initial density operator is that of a free field thermal *quantum* ensemble (cf. appendix A in [17]),

$$\hat{\rho} = \prod_k \int d\varphi_k d\pi_k p_k(\varphi_k, \pi_k) |\varphi_k, \pi_k\rangle \langle \varphi_k, \pi_k| \propto e^{-\hat{H}_0/T_0}. \quad (12)$$

It should be stressed that this ensemble is not in equilibrium, even though the particle densities we compute from the initial conditions (after averaging over a large number of realizations) have a BE distribution. This is clear, because the mode functions do not contribute at all to the initial particle density. In each individual run we therefore expect quick excitation of the mode functions from their vacuum state, i.e. quantum particles will be created, using energy from the mean field. Moreover we use the free field dispersion relation $\omega_k^2 = m^2 + [2 - 2\cos(ak)]/a^2$ in the initial distribution (11), with the zero temperature mass $m \equiv m(0)$. In thermal equilibrium this should become the temperature dependent mass $m(T)$ of the quasi-particles. Nonetheless we expect that these initial conditions will lead to a much faster thermalization than initial conditions of the form (10).

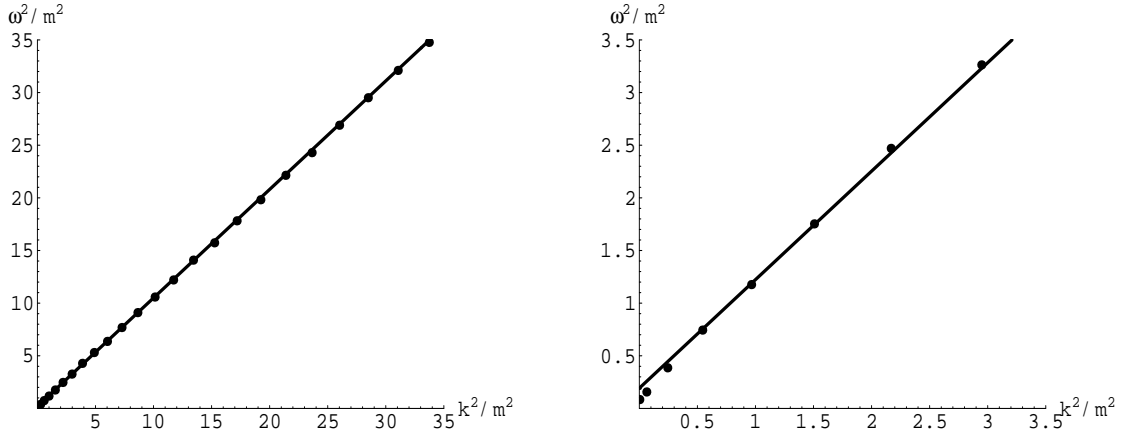


Figure 1: Dispersion relation computed from a Monte Carlo simulation of the euclidean time version of the model. The model parameters are: $\lambda/m^2 = 1/2v^2 = 1/4$, $Lm = 25.6$, $1/am = 10$ and $T/m = 1$, with 20 steps in the euclidean time direction. Here k is the lattice momentum $\sqrt{2 - 2 \cos(ak)}/a$. The statistical error bars are smaller than the symbols. The right figure is a zoom-in at small k where deviations from linear behavior are visible.

3 Monte Carlo check

To study time-dependence of particle energies and densities we define energies ω_k and densities n_k from the Fourier components of the $\hat{\varphi}$ and $\hat{\pi}$ two-point functions,

$$\begin{aligned} \frac{1}{L} \sum_{xy} e^{-ik(x-y)} S_{xy} &= (n_k + \frac{1}{2})/\omega_k, \\ \frac{1}{L} \sum_{xy} e^{-ik(x-y)} U_{xy} &= (n_k + \frac{1}{2})\omega_k, \end{aligned} \quad (13)$$

where U_{xy} is similarly defined as S_{xy} in (8), with φ replaced by π . For weakly coupled fields one expects the equilibrium particle densities defined in this way to have a Bose-Einstein distribution, and energies to have a free quasi-particle dispersion relation, approximately,

$$n_k = (e^{\omega_k/T} - 1)^{-1}, \quad \omega_k^2 = m(T)^2 + [2 - 2 \cos(ak)]/a^2. \quad (14)$$

The effective mass $m(T)$ of the quasi-particles is temperature dependent. In the following we shall use the zero temperature mass $m \equiv m(T = 0)$ to scale dimensionful quantities.

To substantiate this expectation (14), we have performed several Monte Carlo simulations of the euclidean time version of our model at parameter values in the same range as we use for the Hartree simulations. In Fig. 1 we show the dispersion relation computed from such a Monte Carlo simulation. We chose a temperature $T/m = 1$ and measured

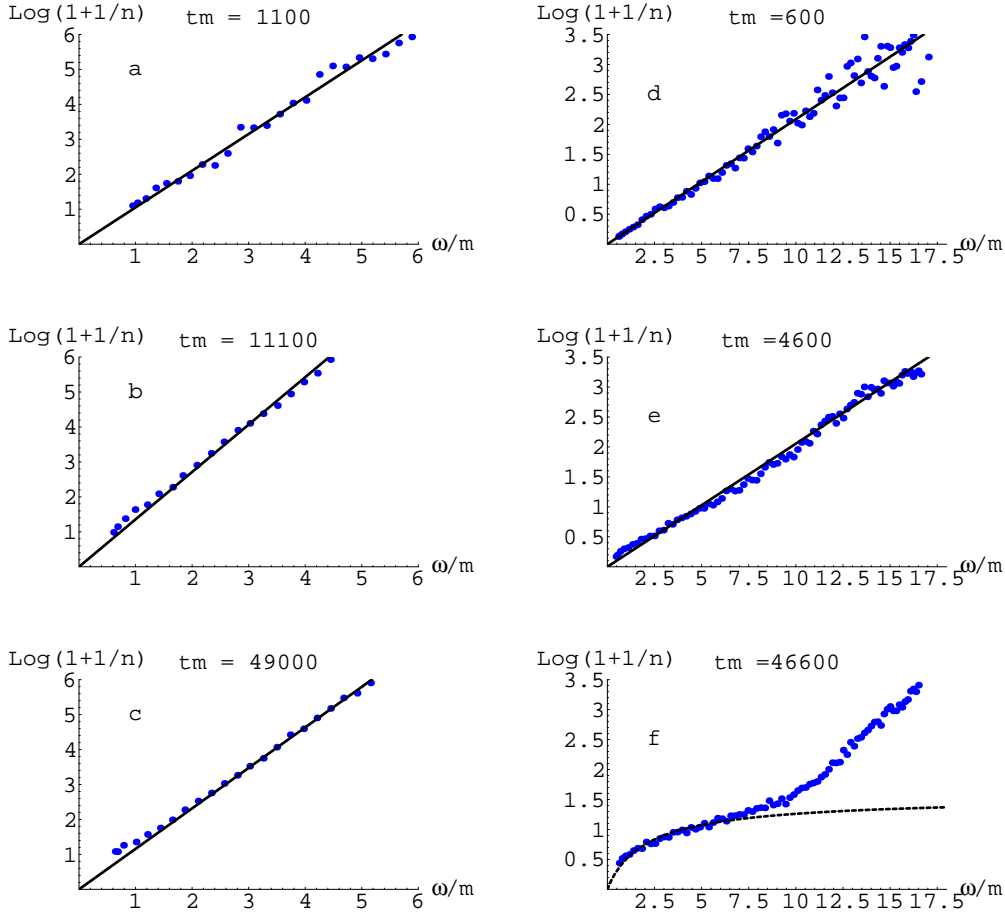


Figure 2: Particle densities as a function of energy, plotted as $\log(1 + 1/n)$. In Figs. a-c on the left the initial $T_0/m = 1$; on the right the initial temperature is high, $T_0/m = 5$. The model parameters are: $\lambda/m^2 = 1/2v^2 = 1/12$, $Lm = 25.6$, $1/am = 10$.

S_{xy} . We stress that such a Monte Carlo simulation gives the *exact* (up to statistical errors) results for the finite temperature Green function. Making the assumption that n_k has the BE form, we computed the ω_k from S_{xy} using (13). As can be seen from the figure, the free form (14) for the quasi-particle dispersion relation holds very well, with $m(T)/m \approx 0.43$. This value is close to that found with the effective potential calculations in the Hartree approximation [17], which gives $m(T)/m \approx 0.41$ at $T/m = 1$ (see also Fig. 3). The effects of the temperature and interactions show up almost exclusively in the value of the effective mass $m(T)$.

4 Weak coupling

In our previous work, using the far out-of-equilibrium initial conditions (10), we found that particles of increasingly higher energy are created and acquire densities with a BE distribution. However, this thermalization progressed rather slowly to high energies, such that the low momentum particle densities already started to deviate from a BE distribution before particles with energies of a few times the temperature could participate in the equilibrium. These two phenomena – particles being created with densities that have a BE distribution and the gradual emerging of equipartition-like features – will be investigated below using the thermal initial conditions (12).

To probe the large time behavior we shall use stronger coupling and higher energy densities than in our previous work. However, first we show results at the same coupling as used in [17]. The coupling constant $\lambda/m^2 = 1/2v^2 = 1/12$ is in the “broken symmetry phase” of the model. The volume $Lm = 25.6$ and the lattice cut-off $1/am = 10$.

We plot $\log(1+1/n_k)$ rather than n_k itself, because in this way a BE distribution shows up as a straight line with a slope equal to the inverse temperature. The scattering in the data points is due to using only a few Hartree realizations (only two initial conditions). At low temperature, $T_0/m = 1$, Figs. 2a-c, the evolution is very slow and there is hardly a sign of emerging classical features even at the largest time $tm \approx 50000$. Even though the particle distribution does not change, there is a persistent, slow transfer of energy from the mean field into the modes. At $tm = 200$, 50% of the energy is still in the mean field, at $tm = 6000$ this has dropped to 25% and at $tm = 50000$ it is still some 15%. The effective mass stays roughly constant, $m(T)/m \approx 0.94$, which is consistent with the effective potential for $T_0/m = 1$.

At higher temperature, $T_0/m = 5$, but with the same weak coupling, there is again a wide window in which the particles have a BE distribution without significant distortions (Figs. 2d-f). However, we see classical-like features emerging for $tm \gtrsim 4000$: compared to the BE distribution, the low momenta modes become under-occupied, while the high momenta modes become over-occupied. We find that at the latest time $tm \approx 50000$ the distribution for $\omega/m \lesssim 7$ can be described reasonably well with an ansatz $n_k = c_0 + T_{cl}/\omega_k$. Without the constant $c_0 \approx 0.25$ the fit would be poor.

In this simulation we find an interesting behavior of the effective mass, shown in Fig. 4. For comparison, we also show in Fig. 3 the effective mass calculated using the Hartree effective potential at the same model parameters. First the mass is steadily decreasing, which is appropriate when the temperature is decreasing and the system is in the hot, symmetric phase. At $tm \approx 14000$ there is a sharp turnover and the mass starts to increase as in the cold, broken phase. The temperature at that point $T_{cl}/m \approx 1.6$, obtained from a classical fit, is close to the temperature $T_c/m = 1.8$ of the first order phase transition computed from the effective potential.[¶] Also the average mean field fluctuates around zero before and around $v \approx 1.8$ after the transition, reasonably close to the effective potential prediction $v \approx 2$ for $T/m \sim 1.6 - 1.8$. The reasonable quantitative agreement between the simulation, which shows classical features, and the effective potential computation, which

[¶] We recall that in the exact theory there would be a cross-over instead of a first order phase transition.

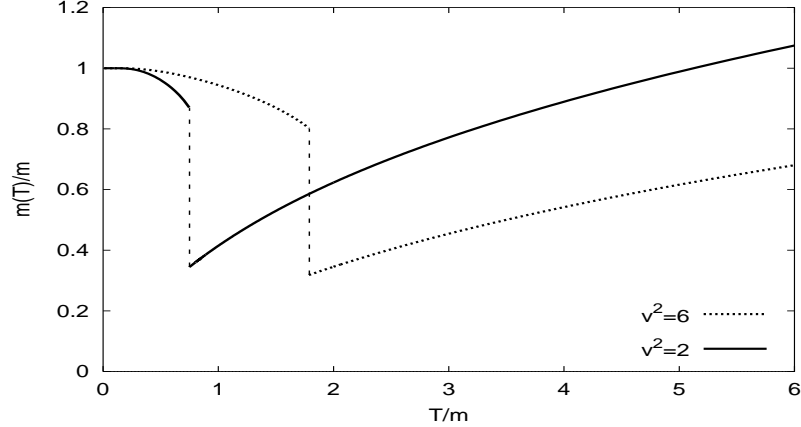


Figure 3: *Temperature dependence of the effective mass computed using the Hartree effective potential [17], $\lambda/m^2 = 1/4$ (solid line) and $1/12$ (dotted line), $mL = 16$ (volume dependence is very small).*

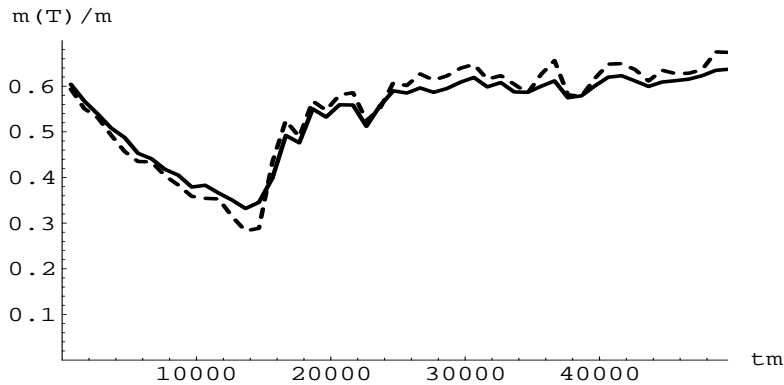


Figure 4: *Time dependence of the effective mass $m(T)$ for the same model as shown in Figs. 2d-f. The mass is determined as the lowest energy ω_0 (dotted line) or from a quadratic fit to the dispersion relation (full line).*

assumes a BE distribution, illustrates that the thermal mass is dominated by the low-energy particles, for which there is little difference between a BE and classical distribution.

5 Stronger coupling

We now turn to the stronger coupling $\lambda/m^2 = 1/2v^2 = 1/4$, in order to make processes evolve faster. In Fig. 5a we show particle densities n_k computed only from the mode functions. We ignore the contribution from the mean field in (8), because we want to focus on the particles described by the mode functions. In Fig. 5a one sees that already after a short time, $tm \gtrsim 10$, particles have been created over a wide range of energies, $\omega/m \lesssim 6$. The densities are reasonably well described by a BE distribution with a time

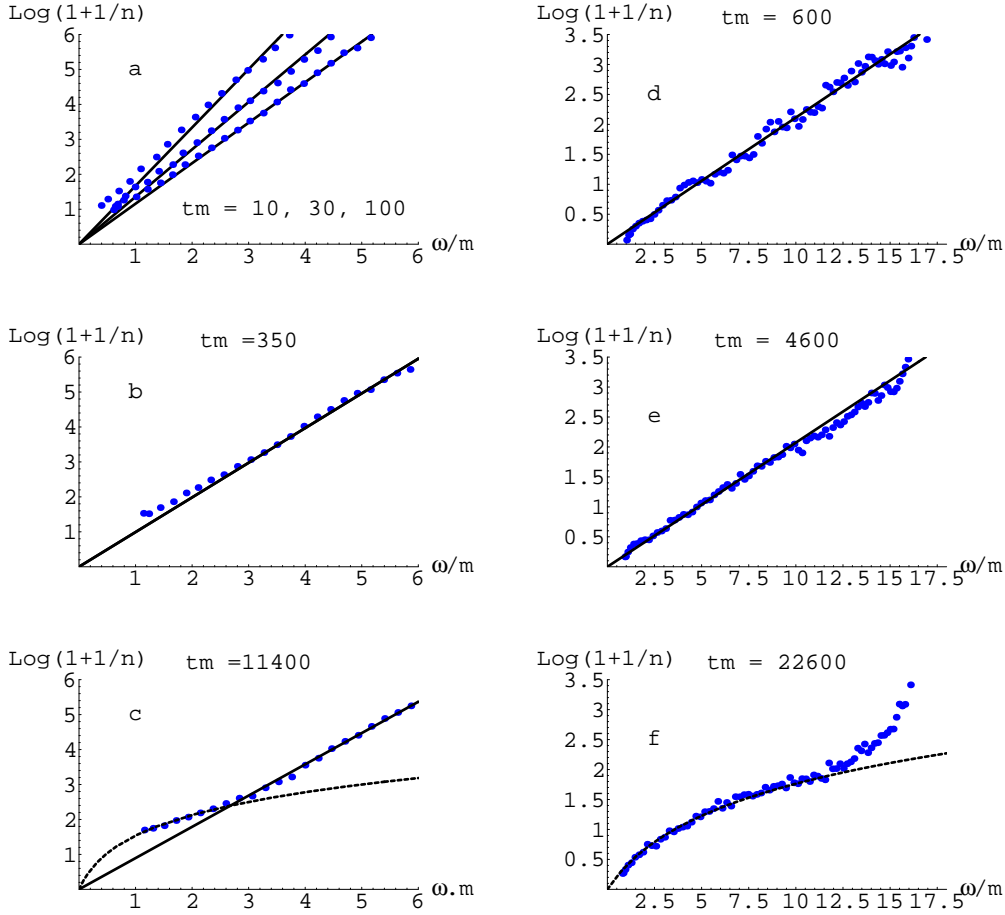


Figure 5: *The same as Fig. 2, but at a stronger coupling $\lambda/m^2 = 1/4$.*

dependent temperature. This temperature initially increases rapidly from $T/m = 0$ at $tm = 0$ to $T/m \approx 0.6$ at $tm = 10$ and then gradually increases further to $T/m \approx 0.9$ at $tm = 100$. (Recall that the temperature of the initial condition is $T_0 = m$.)

Figs. 5b-c, which are obtained using both the modes and mean fields to compute the correlation functions, show that the densities of particles with large momenta tend to remain at a BE distribution also for later times, with a very slowly increasing temperature $T/m = 0.93 - 1.13$. However, one also clearly sees deviations from the BE distribution developing, starting at the low ω -side of the spectrum.

From these data we infer two time scales: First there is the rate at which the temperature of the BE distribution of the quantum particles is established. Second there is a rate at which the classical-like distribution sets in. Fig. 6 shows the time dependence of these two processes. The BE temperature was computed by fitting $\log(1 + 1/n) = \omega/T$ (only using the mode function contribution) for $2 \lesssim \omega/m \lesssim 4$. The classical temperature was found from fitting $n = T_c/\omega$ for $\omega/m \lesssim 2$. The time dependence of these temperatures is reasonably well described by an exponential approach to an equilibrium

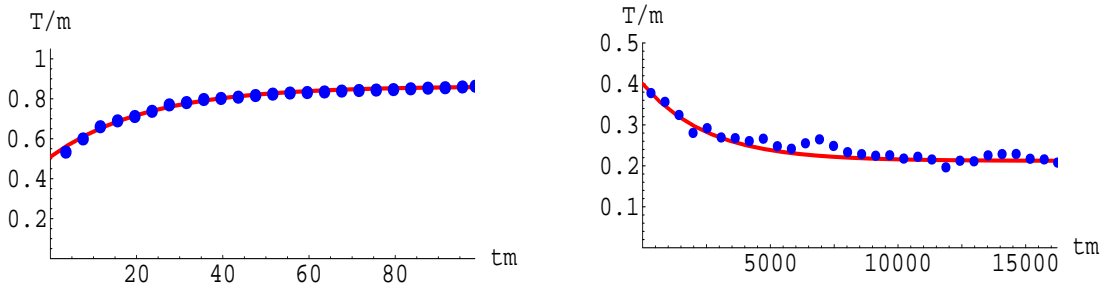


Figure 6: *Time dependence of BE (from the modes only) and classical (from the modes and mean field) temperatures for the data of Figs. 5a-c.*

value, $T_{BE}(t) = A - Be^{-t/\tau_{BE}}$ and $T_{cl}(t) = A' + B'e^{-t/\tau_{cl}}$. We find $m\tau_{BE} \approx 20$ and $m\tau_{cl} \approx 2500$, showing quantitatively that the approximate BE thermalization happens much faster than the emergence of classical-like behavior (Note that T_{cl} becomes much lower than T_{BE} , which itself is somewhat smaller than T_0 , in agreement with the eventually expected classical equipartition).

At higher temperature, the distribution roughly follows the same development. Surprisingly enough the distribution keeps its approximate BE form much longer, while at a higher temperature one expects a stronger effective coupling, and thus shorter time-scales. In Figs. 5d-f the initial temperature is $T_0/m = 5$. At this higher temperature and on a correspondingly larger energy scale, the deviations from a BE distribution appear less pronounced at early times. But even at $tm = 4600$ the particle densities are reasonably well described by a BE distribution with a temperature $T/m \approx 4.8$. At this time, there is a small reduction of the density of low momentum particles (n is up to 15% smaller than the BE density, which is hard to see on the log-plot). At the same time the density of particles, with ω/m in the region 10 – 12, increases a little. This trend continues and at $tm = 22600$ there is classical behavior for $\omega/m \lesssim 12$.

The dashed line in Fig. 5f is a fit of the form $n = T_{cl}/\omega$, which gives a “classical” temperature $T_{cl}/m \approx 2.1$. The good quality of this fit for $\omega/m \lesssim 12$ suggests that the BE distribution gradually turns over into classical equipartition. However, for still larger times the distribution is no longer well described by a simple $n \propto 1/\omega$ -dependence. We did not determine the final equilibrium distribution, because of the extremely long (computer) time this would require.

In Table 1 we summarize our results for τ_{BE} and τ_{cl} , including also fits to the time dependence of the particle density $\sum_k n_k$, computed from the modes only or mean field plus modes, as in Figs. 6. These results do not show a clear dependence on the coupling or temperature, contrary to the expectation of much smaller time scales at higher temperature and/or stronger coupling. We believe that this is accidental, due to the fact that at $T_0/m = 5$ and/or $\lambda/m^2 = 1/4$ the system is in the “symmetric phase”, while it is in the “broken phase” for $T_0/m = 1$ and $\lambda/m^2 = 1/12$. We have noticed previously [17] that in the “symmetric phase” the system evolves much more slowly than in the “broken phase”. Note that the numbers in the table are subject to systematic uncertainty, since

λ/m^2	1/12		1/4	
T_0/m	1	5	1	5
$m\tau_{BE}$	35	35	25	25
$m\tau_{cl}$	> 15000	3000-5000	2500-3500	2000-5000

Table 1: *Results for the BE equilibration time, τ_{BE} , and the time scale for the drift towards classical equipartition, τ_{cl} , obtained from fits to T_{BE} and T_{cl} as in Fig. 6, as well as similar fits to the time dependence of $\sum_k n_k$.*

the mode system starts far from equilibrium and the time dependence not always follows an unambiguous exponential relaxation. This applies in particular for the simulation at $\lambda/m^2 = 1/4$, $T_0/m = 1$, which is very close to the “phase transition”.

Besides looking at the particle number distribution, it is interesting to follow the effective mass $m(T)$ in time. Comparing it with the temperature dependence computed analytically using the Hartree effective potential [17], gives another measure for the effective temperature of the system. The simulation of Figs. 5a-c gave an effective mass which increased slightly in the range $m(T)/m = 0.84 - 0.89$. From the effective potential calculation we then infer that the temperature should be in the range $0.5 \lesssim T/m \lesssim 0.7$, i.e. in the “low temperature” phase of the model, cf. Fig. 3, which is confirmed by checking the values of the mean field. This temperature is considerably lower than the BE temperature $T/m = 1.0(1)$ estimated from the particle distribution at higher momenta, but is consistent with the temperature obtained from fitting n_k at the smaller ω_k with a classical distribution. The same is found for the high-temperature simulation of Figs. 5d-f: $m(T)/m$ decreases from 1.12 at the start to 0.60 at $tm = 22600$, which corresponds, using the effective potential, to a decrease from $T/m \approx 5$ to $T/m \approx 2$, consistent with the observed $T_{cl}/m \approx 5$ to $T_{cl}/m \approx 2.1$. As mentioned before, the difference between the classical and BE distribution is unimportant for the dominant n_k , those at low momenta.

6 Reduced number of mode functions

If the positive results for the performance of the Hartree ensemble method at shorter times carry over to more realistic models in $3 + 1$ dimensions, one has to confront the problem of the high computational cost of this approach. Taking the continuum limit on a finite volume in d dimensions, i.e. increasing the number of lattice sites N in each direction, the cost of our approach increases $\propto N^{2d+1}$: There are $O(N^d)$ fields which have to be updated $O(N)$ times, assuming a fixed value of the time-step a_0/a .

Most of this cost comes from having to solve all N^d mode functions f^α . However, many of these modes would represent particles with very high momenta $|k| \gg T$. Such particles have very low densities and should be irrelevant for the physics at lower scales. This suggests reducing the number of mode functions in our simulations. We have tested this idea by comparing a simulation on a lattice with $N = 128$ sites using all 128 mode

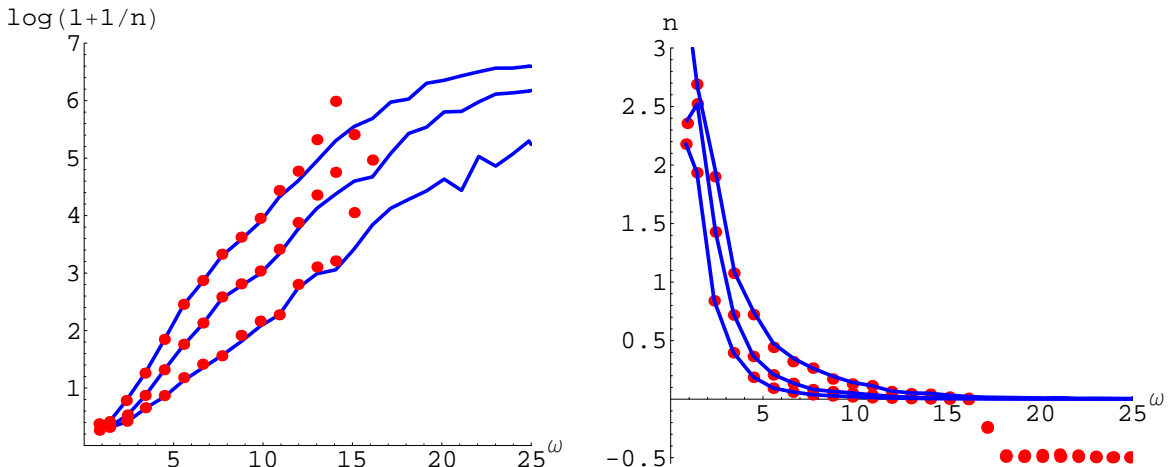


Figure 7: Particle densities at $tm = 50, 90, 300$, obtained from simulations using the full number of modes (drawn lines) and using only modes for which $\omega_k/m < 17 \approx 3T/m$. The left figure shows $\log(1+1/n)$, the right shows the density n itself ($Lm = 5.7$, $1/am = 22.3$ and $\lambda/m^2 = 1/12$).

functions, with the same simulation using only 32 mode functions. This induces a maximum energy $\omega_{\max}/m \approx \sqrt{2 - 2 \cos(32\pi/128)}/am \approx 17$, which is much larger than the temperature $T/m \approx 6.8$ that we will use in the test. The ω_{\max} here refers to the energy of the initial mode functions which are plane waves.

In order to make as detailed a comparison as possible, we show the results for the particle density obtained from the mode functions only, leaving out the contribution of the mean field in (8). As shown in Fig. 7, this partial distribution changes with time during thermalization (cf. Fig. 5a). The drawn lines represent the data obtained with the full number of mode functions. The dots represent the results obtained using the reduced number of modes. The left figure shows the familiar $\log(1+1/n)$ form of the density, the other figure shows the density n itself. As is evident, these results reproduce the data from the reference simulation accurately up to $\omega/m \approx 12$, which is close to $\omega_{\max}/m \approx 17$. Notice that the densities, computed from eq. (13), drop to $n = -0.5$ for $\omega/m \gtrsim 17$ (Fig. 7 right). For these high momenta there are no more mode functions available to provide the vacuum fluctuations that should lift the density to zero. It indicates that at high momenta there is still a roughly one-to-one correspondence between mode functions and momentum labels of the particles.

7 Classical approximation

Even using fewer mode functions, the Hartree approach is much more expensive than the classical approximation (which has no mode functions). So it is important to check if our results cannot in some way be mimicked by a classical approximation. The standard way to implement the latter at high temperature, is to average over initial configurations drawn

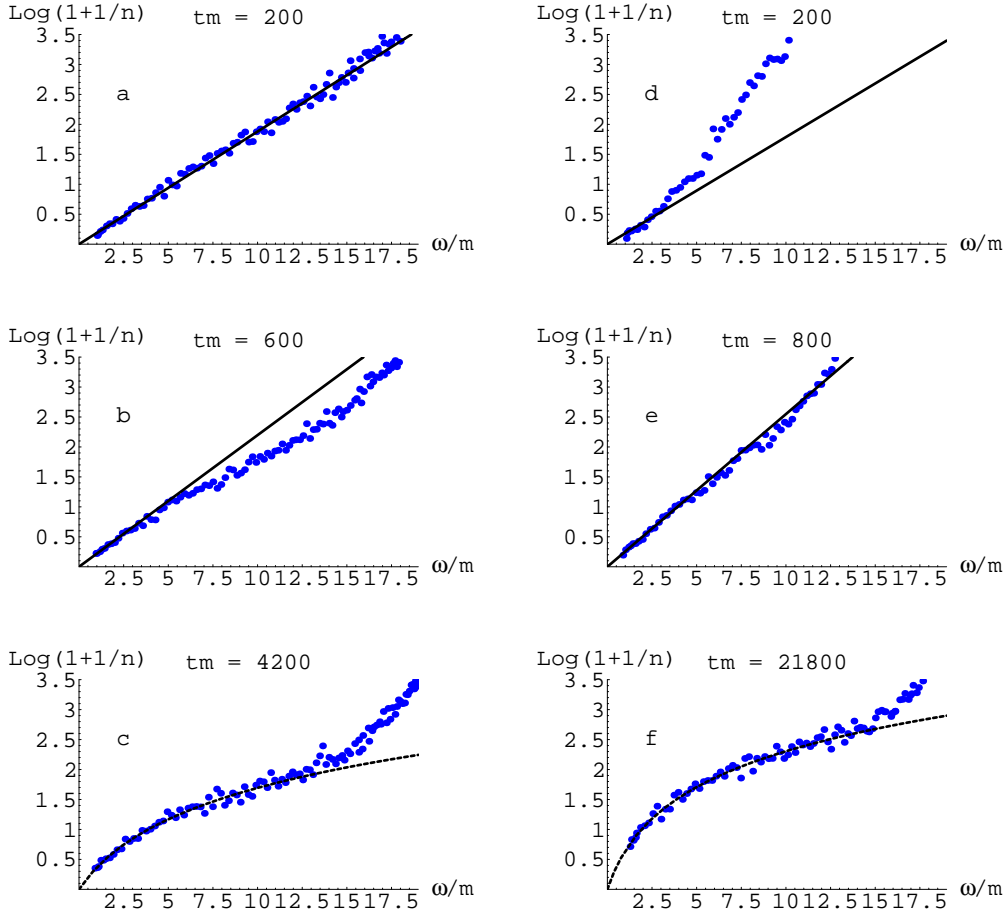


Figure 8: Same as Figs. 5d-f, but using classical dynamics. Figs. a-c have BE-type initial conditions with temperature $T_0/m = 5$, in Figs. d-f only a few of the low momentum modes of the mean field carried all energy. The other model parameters are: $\lambda/m^2 = 1/4$, $Lm = 25.6$ and $1/am = 10$.

from the Boltzmann distribution. Up to modifications by the interactions this implies a classical distribution function $n(\omega) = T/\omega$, with a slow fall off causing Rayleigh-Jeans type divergences. Actually, in $1 + 1$ dimensions such divergences are absent in $\varphi\varphi$ -correlation functions [2].

Here we want to ask a somewhat different question: to what extent can classical dynamics be used to represent a thermalized system with a Bose-Einstein distribution for the particle densities? To investigate this we shall use the same BE-type initial conditions (11) as in the Hartree case, as well as the much more out-of-equilibrium conditions of the form (10). We perform similar simulations and analyses as before, but now without mode functions (and with $n_k + 1/2 \rightarrow n_k$ in (13), as there is now no quantum vacuum contribution). Typically, the classical dynamics produces data with more noise, since the average contribution of the many mode functions tends to smoothen results in the Hartree-

dynamics. We counter this noise by averaging over 40-50 initial conditions, which is much more than we typically use with Hartree dynamics. We note in passing that the necessity to use a larger ensemble to obtain data of the same quality as with Hartree dynamics, diminishes the computational advantage of using classical dynamics considerably.

At the same weak coupling and low temperature as in Figs. 2a-c, we find that the classical system also preserves the Bose-Einstein distribution of the initial conditions very well. Even at the largest simulated time, $tm = 50000$, there is no compelling sign of equipartition in the particle distribution. This, however, may only show that the relaxation time-scale of the classical dynamics is very long, cf. [8], and that we are seeing remnants of the initial condition rather than thermalization.

To speed-up the dynamics we increased the temperature to $T_0/m = 5$ and the coupling to $\lambda/m^2 = 1/4$, as was used in Figs. 5d-f. The results are shown in Figs. 8a-c. Now the initial BE-distribution still persists for some time, but already at $tm \approx 600$ there are clear signs of equipartition setting in, whereas effects of similar magnitude only emerged at $tm \gtrsim 6000$ with Hartree dynamics. The gradual move from the initial state towards classical equipartition happens much faster than in the Hartree ensemble simulations.

Of course one might argue that this initial persisting of the BE distribution is of little significance, since it only demonstrates that it takes time to lose the effect of the initial conditions. In more realistic models we might not be able to specify initial conditions sufficiently close to thermal equilibrium and then one may not expect to encounter a BE distribution. Yet, somewhat surprisingly, starting with the far out-of-equilibrium initial condition (10), we see that as the model steadily moves towards classical equipartition, the particles are distributed in a BE-like way in an intermediate stage. This can be seen in Figs. 8d-f, where we show particle density distributions at simulation times in the range $tm = 200 - 20000$. At tm around 800 the particle densities follow a BE-like distribution over a wide range of energies. The coupling strength in this simulation is $\lambda/m^2 = 1/4$, at weaker coupling this intermediate stage with BE-like distribution persists longer. However, it always smoothly turns towards classical equipartition on much shorter time-scales than when using Hartree dynamics (although, as mentioned above, the final equilibration to the classical distribution takes place on a very long time scale).

8 Discussion

Using Monte Carlo methods we checked that the quasi-particle assumption, which is basic to our definition of the particle distribution function, is well satisfied in the range of couplings and temperatures considered here and in [17].

From the results in this work combined with [17], the following picture has emerged for the 1+1 dimensional $\lambda\phi^4$ model in the “broken phase”. The initial energy, which is put solely in the mean field of a realization, is subsequently transferred to the mode functions. This process takes place fairly locally in momentum space, i.e. mean field modes with momentum k excite primarily particle modes with momenta close to k , and the modes then thermalize locally to a BE distribution. In our previous work this approximate thermalization was more conspicuous because the initial distribution was further out of

equilibrium. Here the BE distribution was put into the initial condition for the mean fields. However, the corresponding density operator is still out of equilibrium because of the “wrong” initial thermal mass. The thermalization process is fairly rapid, within a time $\tau_{BE} \approx 25 - 35 m^{-1}$, for $\lambda/m^2 = 1/4, 1/12$ and $T_0/m = 5, 1$, as determined from the time-dependence of the BE temperature or the particle density $\sum_k n_k$ (cf. Table 1).

This time scale is similar to our findings with initial mean fields containing only low momenta [17]. The subsequent thermalization of higher momenta is very slow. We ascribe this to a weakening of the non-linearities when the mean field loses much of its energy. When the mean field fluctuates around its (temperature dependent) equilibrium value, with diminishing amplitude, the dynamics becomes approximately that of Hartree with a homogeneous mean field, suggesting lack of thermalization. This also explains why the evolution to a classical-like distribution is much slower with the Hartree ensemble approximation than using classical dynamics.

However, the fluctuations die out very slowly and even at very large times of order $10^4 m^{-1}$ there is still $O(10\%)$ of the energy in the fluctuating mean field. Nonlinear fluctuations remain, which lead eventually to classical-like equipartition (according to the effective hamiltonian and conserved “charges” [17]).

The time scale for such classical equipartition setting in could not be determined in [17], its determination is one of the results of the present work. We find that the system remains in an approximate quantal thermal state for times of the order $\tau_{cl} \gtrsim 100 \tau_{BE}$ (cf. Table 1).

This is an encouraging result. For example, in a crude application of our 1+1 dimensional results to 3+1 dimensional heavy ion collisions, identifying m with the mass of the σ -resonance $m_\sigma = 600 - 1200$ MeV, say 900 MeV, a time-span of $100 \tau_{BE} = 2000 m^{-1}$ would correspond to a reasonable length of about 450 Fermi. Within such a time-span the Hartree ensemble method may be a definite improvement on the classical dynamics usually employed for e.g. the “disoriented chiral condensate”.

For application to 3+1 dimensions it is important that the numerical efficiency of the Hartree method can be significantly improved by using only a limited number of mode functions, corresponding to particles with sufficiently high densities (see sect. 6).

Leaving out the mode functions altogether, i.e. using classical dynamics, the results were qualitatively similar to those with Hartree dynamics, but the emergence of classical particle distributions goes faster by roughly an order of magnitude. So this may not be good enough for practical applications.

With respect to thermalization it is good to keep in mind that in the Boltzmann approximation, the collision term corresponding to $2 - 2$ scattering is identically zero, due to kinematical constraints in the φ^4 model in 1+1 dimensions. So thermalization has to come from inelastic scattering and/or off-shell effects. It is then important to realize that such effects are more pronounced in the “broken phase” of the model, which has a three point vertex and finite (as opposed to zero) range interactions. As mentioned in [17], thermalization is drastically less efficient in the “symmetric phase” at similar values of λ/m^2 . It is sobering to recall the huge thermalization times found in [8] in the classical approximation, in the “symmetric phase”. For example, using $\lambda/m^2 = 1/4, T/m = 0.2$,

the formula (rewritten in our conventions) $1/m\tau_{\text{class}} = 5.8 \cdot 10^{-6} (6\lambda T/m^3)^{1.39}$ found in this work leads to a relaxation time $m\tau_{\text{class}} \approx 1.3 \cdot 10^5$. This is much larger than the $m\tau_{cl} \approx 2500$ found here in the “broken phase” (Sect. 5).

An interesting question is how the two time scales τ_{BE} and τ_{cl} are related to particle scattering and damping. A perturbative computation (which includes direct scattering through the setting-sun diagram), indicates that the damping time would be of the order of the BE-relaxation time τ_{BE} (i.e. much shorter than the relaxation time away from BE behavior). Preliminary numerical results for the damping time are consistent with these values [18, 19].

This is a favorable result for the Hartree ensemble method. However the gradual drift away from a BE distribution and the corresponding cooling of the system reveals a shortcoming. This is additional to the incorrect prediction by the Hartree method, of the order of phase transitions. Further improvements are needed, in particular if large time scales are to be investigated.

Acknowledgments

We thank Gert Aarts for useful comments. This research was supported by FOM/NWO.

References

- [1] G.D. Moore and K. Rummukainen, Phys. Rev. D61 (2000) 105008, hep-ph/9906259,
- [2] W.H. Tang and J. Smit, Nucl. Phys. B540 (1999) 437, hep-lat/9805001,
- [3] S.Y. Khlebnikov and I.I. Tkachev, Phys. Rev. Lett. 77 (1996) 219, hep-ph/9603378,
- [4] T. Prokopec and T.G. Roos, Phys. Rev. D55 (1997) 3768, hep-ph/9610400,
- [5] G. Felder and L. Kofman, Phys. Rev. D63 (2001) 103503, hep-ph/0011160,
- [6] J. García-Bellido et al., Phys. Rev. D60 (1999) 123504, hep-ph/9902449,
- [7] A. Rajantie, P.M. Saffin and E.J. Copeland, Phys. Rev. D63 (2001) 123512, hep-ph/0012097,
- [8] G. Aarts, G.F. Bonini and C. Wetterich, Phys. Rev. D63 (2001) 025012, hep-ph/0007357,
- [9] G. Aarts and J. Smit, Nucl. Phys. B511 (1998) 451, hep-ph/9707342,
- [10] G. Aarts and J. Smit, Phys. Lett. B393 (1997) 395, hep-ph/9610415,
- [11] F. Cooper et al., Phys. Rev. D50 (1994) 2848, hep-ph/9405352,
- [12] D. Boyanovsky and H.J. de Vega, (2000), astro-ph/0006446,

- [13] B. Mihaila et al., Phys. Rev. D62 (2000) 125015, hep-ph/0003105,
- [14] J. Berges and J. Cox, (2000), hep-ph/0006160,
- [15] L. Mandel and E. Wolf, Optical coherence and quantum optics (Cambridge University Press, 1995).
- [16] J.R. Klauder and B.S. Skagerstam, Coherent States (World Scientific, 1985).
- [17] M. Sallé, J. Smit and J.C. Vink, Phys. Rev. D64 (2001) 025016, hep-ph/0012346,
- [18] M. Sallé, J. Smit and J.C. Vink, (2000), hep-ph/0008122,
- [19] M. Sallé, J. Smit and J.C. Vink, Nucl. Phys. Proc. Suppl. 94 (2001) 427, hep-lat/0010054,